ELSEVIER

Journal of Hazardous Materials A126 (2005) 8–13

Journal of Hazardous Materials

www.elsevier.com/locate/jhazmat

Force analysis and visualization of NAPL removal during surfactant-related floods in a porous medium

Seung-Woo Jeong [a,*], M. Yavuz Corapcioglu [b]

[a] *Department of Environmental Engineering, Kunsan National University, Kunsan 573-701, Republic of Korea*
[b] *Department of Civil Engineering, Texas A&M University, College Station, TX 77843, USA*

Received 11 January 2005; received in revised form 27 May 2005; accepted 8 June 2005
Available online 27 July 2005

Abstract

Governing mechanisms of dense non-aqueous phase liquid (DNAPL) removal during surfactant and surfactant-foam (SF) flooding were studied by porous-patterned glass model experiments. Physical forces, viscous forces and capillary forces, acting on trichloroethylene (TCE) blobs were quantified to understand DNAPL removal mechanisms during the floods, simultaneously visualizing the removal mechanisms. The viscous force of the remedial fluid was intimately related to TCE removal from the porous medium. The remedial fluid with a high viscous force displaced more TCE blobs. Displacement of residual TCE by the remedial fluid began as viscous pressure of flooding was closed to the capillary pressure of the porous medium. In the region of viscous pressure less than the capillary pressure, residual TCE was either retained or solubilized, not displaced, implying that TCE solubilization was the dominant TCE removal process. Glass porous model visualization validated a dominance of the capillary forces during a surfactant flush and a dominance of the viscous forces of the displacing fluid during a SF flood.

Keywords: Surfactant; Surfactant-foam; DNAPL; Viscous force; Capillary force

1. Introduction

Trichloroethylene (TCE) is the most frequently detected groundwater contaminant at hazardous waste sites [1]. As the free product moves downward as a separate phase after an initial non-aqueous phase liquid (NAPL) spill or leak, it leaves behind a residual phase trapped in the aquifer material by capillary forces [2]. The prevalence of NAPLs is a significant impediment to the cleanup of aquifers. Surfactant flushing has been recognized as an efficient technology for the remediation of aquifers contaminated with NAPLs. A surfactant-enhanced remediation technique is used to enhance NAPL solubility and/or mobilize NAPL ganglia by reducing the interfacial tension (IFT) between the organic phase and the aqueous phase [3,4].

The mobilization of dense NAPL (DNAPL) by lowering the IFT has been discouraged since this approach may cause the trapped DNAPL to migrate downward, expanding the area contaminated by DNAPL. Fountain et al. [4] recommended applying an IFT greater than 3–5 dyne/cm to avoid inducing the vertical migration of DNAPLs. Unlike most emulsified mobilization schemes significantly reducing interfacial forces, viscous and buoyancy forces are modified or increased for DNAPL mobilization in recent studies. Miller et al. [5] modified buoyancy forces in a DNAPL-contaminated system by using dense brine solutions. Some researchers used polymers to increase viscous force of remedial fluids to enhance displacement efficiency [6,7]. Jeong et al. [8] used surfactant-foam (SF) for TCE displacement in a moderate IFT system of 4.9 dyne/cm. Although it is expected that surfactant-related remediation systems using increased viscous force would displace more organic phase trapped in pores, the increased viscous force has not been quantified with the organic phase desaturation. It is also known that the

* Corresponding author. Tel.: +82 11 9075 3595; fax: +82 63 469 4964.
E-mail address: superjeong@yahoo.com (S.-W. Jeong).

0304-3894/$ – see front matter © 2005 Elsevier B.V. All rights reserved.
doi:10.1016/j.jhazmat.2005.06.015

organic phases trapped in pores would be displaced under the conditions of viscous force greater than the capillary force of the pore. However, those phenomena have not been clearly visualized together with the acting force analysis.

This study quantified the viscous forces of the surfactant-related remedial fluids (i.e., surfactant and SF) and the TCE desaturation, and also visualized displacement of DNAPL at the region of viscous force greater than the capillary force of the porous medium. Therefore, the objective of this study was to construct a relationship diagram of the viscous force of surfactant-related remedial flood and the TCE desaturation. The results would be utilized to determine the dominant removal process during flooding and design an efficient remediation system. This study used a well-defined porous model for physical force analysis and TCE quantification because the physical properties of porous medium can be easily quantified in the well-defined porous medium and relatively accurate TCE saturation can be directly measured by an image analysis technique.

2. Materials and methods

2.1. Measurements and procedures

This study used a well-defined porous medium for physical force analysis of remediation floods. A porous pattern-regularly-etched glass model was allowed us to quantify physical forces and visualize removal phenomena during flooding. The glass model and experimental set-up used in this study were already described in Jeong et al. [8]. Details of the experimental procedure were also given in ref. [8]. Fluid properties used in this study were shown in Table 1. The micromodel was initially saturated with water and then injected with dyed PCE. This resulted in the micromodel being almost saturated with dyed TCE. The micromodel was then flushed by water until only residual NAPL remained. After water flooding was completed, residual TCE saturation (S_{TCE}) was measured as 0.32 ± 0.01. The residual S_{TCE} was quantified by taking pore-scale images and then measuring the TCE blob area.

After 25 pore-volume (PV) flooding, a final S_{TCE} was determined by the ratio of TCE blob area to pore area and was quantified through a direct image analysis [8]. A pressure transmitter monitored the pressure at the injected port and the results were stored in a computer containing data logging software. The results of the pressure variations during 20–25 PV fluid flow were used to determine the average pressure gradient since the pressure variations in this range were small and assumed to represent the steady state conditions.

Table 1
Fluid properties

Fluid	Interfacial tension with red-dyed TCE[b,c]	Viscosity (cP)[d]	Contact angle of TCE[e] (°, TCE phase)
Water	27.3	0.949	147
Surfactant[a]	4.9	1.029	130

[a] Two percent (weight basis) sodium $C_{14–16}$ olefin sulfonate.
[b] Measured by pendant drop method.
[c] Five gram of Oil-Red-O was added to 1 l of TCE.
[d] Measured by a glass tube viscometer.
[e] Contact angle of a TCE blob on the glass was measured by image analyser.

2.2. Viscous and capillary force determination

Three forces, viscous, capillary and gravitational forces, around a NAPL blob is related to the mobilization of NAPL trapped in a porous medium. It is known that the capillary force acts to retain organic phases between the solid grains, while the viscous and gravitational forces contribute to mobilize NAPL blobs. An analysis of these forces acting on NAPL blobs would aid in understanding of the NAPL mobilization. Note that in this study all viscous and capillary forces are expressed as pressures.

2.2.1. Apparent viscosity

Fluid flow in porous media is expressed by Darcy's law, which correlates the flow rate to the potential gradient only if the pore space of the medium occupied with a single Newtonian fluid. Darcy's law has been extended to express the multi-phase flow in porous media by using the relative permeability concept. For a homogeneous isotropic porous medium, Darcy's law is expressed as followed:

$$\boldsymbol{q}_i = -\frac{k_o\, k_{ri}}{\mu_i}\nabla\Phi_i \tag{1}$$

where $\boldsymbol{q}_i$ is the volumetric flux of phase i (i.e., volumetric flow rate per unit area); k_o the intrinsic permeability of the medium; μ_i the viscosity of phase i; k_{ri} the relative permeability of phase i and Φ_i is the potential of phase i, $\Phi_i = P_i + \rho_i g z$, where P_i is the pressure of phase i, ρ_i the density of phase i, g the gravitational acceleration constant and z is the vertical distance. Foam flow in porous media has been described in two different ways. Previous studies described foam as a mixture of two phases (gas and liquid) [9,10] or as a single phase fluid [11,12]. This study treats SF as a single phase fluid and employed the apparent viscosity concept of SF. The apparent viscosity is usually determined by a method strictly applicable to Newtonian fluids [12,13]. Then, for a horizontal micromodel, the apparent viscosity, μ_a can be expressed as:

$$\mu_a = \frac{k_o k_r \nabla P}{\boldsymbol{q}} \tag{2}$$

where ∇P is the pressure gradient. This study used a horizontal micromodel and thus treated the pressure gradient as the potential gradient. The relative permeability, k_r was calculated by Corey's equation [14]. The relative permeability of the foam flow was approximated using the sum of the liquid and gas phase saturations after foam flooding.

2.2.2. Calculation of viscous and capillary pressures

The viscous pressure of the displacing fluid contributes to DNAPL mobilization. The viscous pressure of the displacing fluid (P_V) is obtained as:

$$P_V = \frac{\mu \boldsymbol{q} L}{k_o k_r} \quad (3)$$

where μ is the viscosity of displacing fluid and L is the length of the porous medium. To more clearly represent the effect of the viscosity term on the viscous pressure, this study defined both the applied and produced viscous pressures of displacing fluid, determined by the viscosity term used in the calculations. The applied viscous pressures, $P_{V,app}$ and the produced viscous pressures, $P_{V,pro}$ were calculated by substituting the inherent viscosity of the injecting fluid and the apparent viscosity during flooding in Eq. (3), respectively. Because the apparent viscosity was measured under the actual experimental conditions, it would more accurately and dynamically represent the viscous force of the displacing fluid. At steady-state, $\boldsymbol{q}$ would be equal to the ratio of injection flow rate to unit area in SF flooding because the aqueous phase saturation during foam flooding would be constant within the porous medium [15,16].

The capillary pressure of a porous medium acts to retain NAPLs between the solid grains. The capillary pressure is expressed by the entry capillary pressure to a porous medium, P_C [17]. The entry capillary pressure in the residual TCE system is the pressure of the displacing fluid to penetrate the pore throats of voids TCE occupies. This is defined as:

$$P_C = \frac{2\sigma \cos\theta}{r} \quad (4)$$

where σ is the IFT between two immiscible fluids, θ the contact angle between the two phases on the solid and r is the throat radius of the porous medium (an equivalent radius of 0.0076 cm). The values of σ and θ are given in the measurements and procedures section. TCE was initially entrapped in the pores that were saturated with water. The capillary pressure at the initial TCE entrapment was calculated as 6016 dyne/cm^2 by using the IFT between TCE and water and the contact angle of TCE to water.

3. Results and discussion

3.1. Viscous pressures during surfactant and SF flooding

Fig. 1 presents a comparison of the applied viscous pressure and the produced viscous pressure. A gas fraction (GF) is the ratio of gas (air) volume to SF volume. As mentioned earlier, the applied viscous pressure was calculated by Eq. (3) using the inherent viscosity of the displacing fluid. Because both flood methods (surfactant and SF floods) utilized the same surfactant solution, the applied viscous pressures for both were in the range of 100–10000 dyne/cm^2. However, the produced viscous pressures, which were calculated with

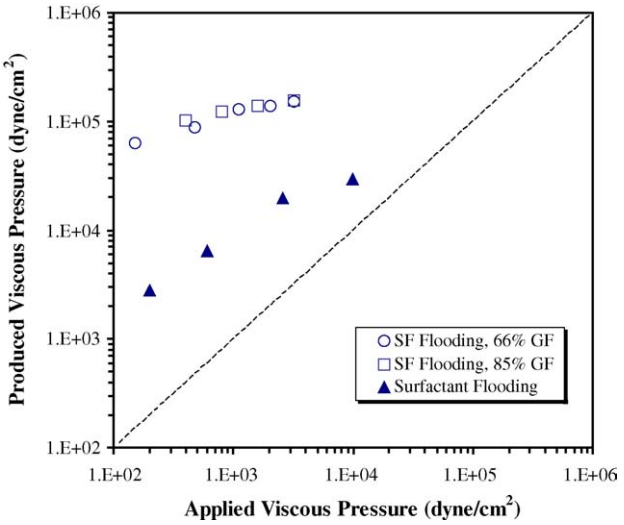

Fig. 1. Comparison of the applied viscous pressure and the produced viscous pressure. The applied and viscous pressures were calculated by Eq. (3) with the inherent viscosity and with the apparent viscosity, respectively. GF is the gas fraction in SF.

the apparent viscosity, showed a large difference between the two flooding methods. While surfactant flooding represented the produced viscous pressures 3–14 times greater than the applied viscous pressures, SF flooding produced viscous pressures 48–414 times greater than the applied viscous pressures.

In a surfactant flood, surfactant solution flowing through TCE trapped pores would become viscous than its inherent property because TCE dissolved into the surfactant solution. The viscous surfactant solution resulted in the higher viscous pressure than the applied (inherent) viscous pressure. The increase in viscous pressures by SF can be explained by the properties of foam flow in porous media. Foam is a homogeneous mixture of surfactant solution and discrete air phase that resembles a bubbly liquid. In enhanced oil recovery (EOR), the apparent viscosity of foam can be up to 1000 times greater than the viscosity of constituent phases; surfactant solution and gas phase [18,19]. In this study, the apparent viscosity of SF was 93 times greater than the constituent phase viscosities. The smaller apparent viscosity of SF stems from much larger bubble size of SF than those of other forms used for EOR. In this study, the average bubble diameter of injected SF was 2.5 mm, which is much coarser than other foams. A fine-textured foam leads to larger flow resistance that contributes to increasing apparent viscosity of bulk foam flowing thorough porous media.

3.2. Determining principal force in surfactant and SF floods

In immiscible displacement, the viscous force of displacing fluid is the principal factor in determining the displacement domain. Lenormand et al. [17] classified immiscible displacement phenomena into three domains. They character-

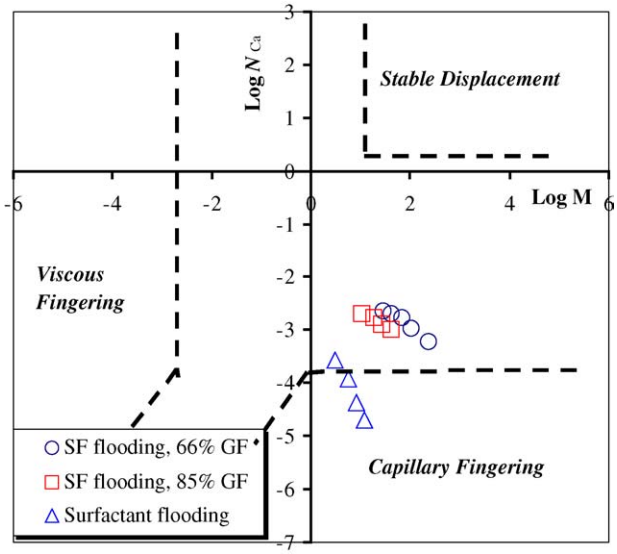

Fig. 2. The displacement phase diagram of immiscible displacement in porous media [17]. M is the viscosity ratio of displacing fluid to the displaced fluid. N_{Ca} is the capillary number, calculated by Eq. (5). Three domains are characterized by dominant displacement behaviors (Reprinted with the permission of Cambridge University Press).

ized the basic forms of displacement using two dimensionless numbers, the capillary number (N_{Ca}) and the viscosity ratio (M) of the displacing fluid to the displaced fluid. Their phase diagram is divided into three predominant domains, i.e., viscous fingering, capillary fingering and stable displacement, and indicated the dominant force during immiscible displacement. While the principle force of the capillary fingering domain is due to the capillary force of the porous medium, the principal forces of the domains of viscous fingering and stable displacement are resulted from the viscosity of the displaced fluid and the displacing fluid, respectively [17]. This study plotted all experiment conditions of surfactant and SF floods on the diagram to determine dominant forces of those floods.

Fig. 2 shows the phase diagram representing the conditions of SF flooding and surfactant flooding. The conditions shown in Fig. 2 were determined from the capillary number (N_{Ca}) of Eq. (5) and the viscosity ratio (M) of the apparent viscosity to the TCE viscosity.

$$N_{Ca} = \frac{\boldsymbol{q}\mu_a}{\sigma \cos\theta} \quad (5)$$

$$M = \frac{\mu_a}{\mu_{TCE}} \quad (6)$$

As shown in Fig. 2, the conditions of surfactant floods mostly corresponded to capillary fingering where the viscous force of the displacing fluid became small and the capillary force of the porous medium was the principal force. Within the capillary fingering domain, all organic phases entrapped in a porous medium would remain stationary. Glass porous model observations validated a dominance of the capillary forces during surfactant floods, revealing that residual TCE

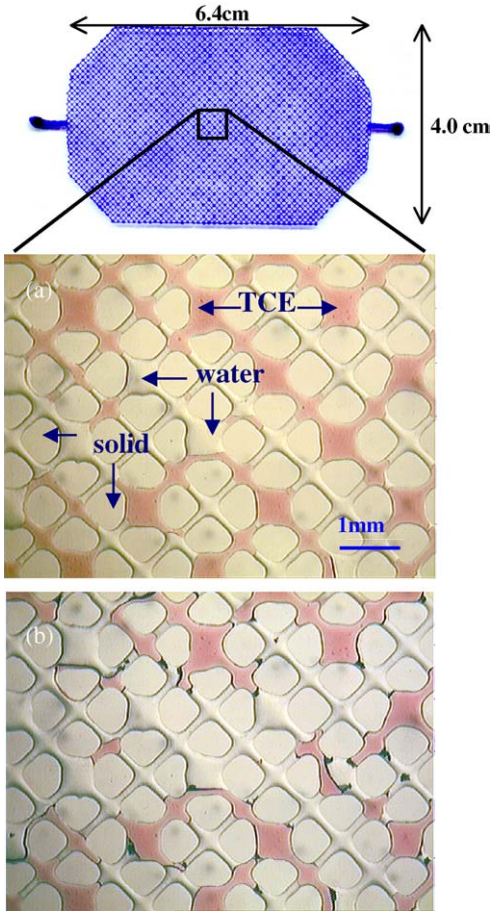

Fig. 3. Images from the porous pattern glass model where the residual TCE was flushed by surfactant solution: (a) the initial image and (b) the final image at 25 pore volume injection.

partially dissolved along the flow channel of the surfactant solution (Fig. 3). The surfactant solution flowed through a preferential flow path dissolving part of the TCE blobs near the channel. The dark area around the residual TCE blobs was the red dye debris left after a portion of the TCE was solubilized. Some residual TCE was either retained or solubilized, not displaced due to capillary force of the porous medium during the surfactant flushing.

The conditions of SF flooding corresponded to the transition zone between the stable displacement and the capillary fingering. The SF flooding conditions shifted from the capillary fingering zone toward the stable displacement zone even though an apparent displacement front was not observed in the glass model visualizations. To obtain a more stable displacement, a higher capillary number would be required by either increasing the Darcy velocity ($\boldsymbol{q}$) or decreasing the interfacial tension (σ). Fig. 4 shows the glass model visualization of SF flooding. Although the surfactant flooding visualizations showed several remaining TCE blobs which were not displaced due to capillary forces, SF flushed most of the trapped TCE due to the increased viscous force of the displacing fluid, as already mentioned in Fig. 1.

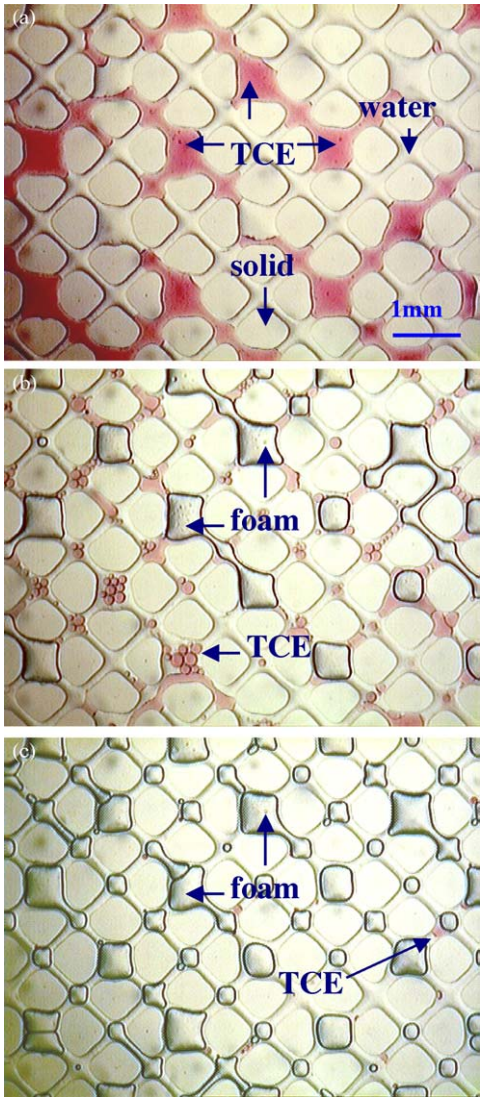

Fig. 4. Images from the micromodel in which the residual TCE was flushed by SF: (a) initial image, (b) 5 pore volume injection and (c) 20 pore volume injection.

3.3. Desaturation of TCE by viscous pressure increment

The S_{TCE} ratio (the ratio of the final S_{TCE} to the initial S_{TCE}) as a function of viscous pressure is shown in Fig. 5. The TCE desaturation is closely related to the viscous pressure. Displacement of the residual TCE by water and surfactant flooding began as the viscous pressure of the flood was closed to the capillary pressure (6016 dyne/cm^2) of the porous medium. A decrease in the TCE desaturation by surfactant flooding is nearly proportional to the decrease by water flooding. This result indicated that the TCE displacement occurred by increasing viscous pressure with increasing the flood velocity. The result also implied that relatively little mobilization of TCE blobs would occur in the region of the viscous pressure less than the capillary pressure of the porous medium, while solubilization would be the dominant removal process in the region. Thus, in the surfactant flood that solubilization was the dominant removal process, the approximate decrease in S_{TCE} ratio by 30% would be attributed to TCE solubilization. However, TCE dissolution by water was negligible in the region close to the capillary pressure.

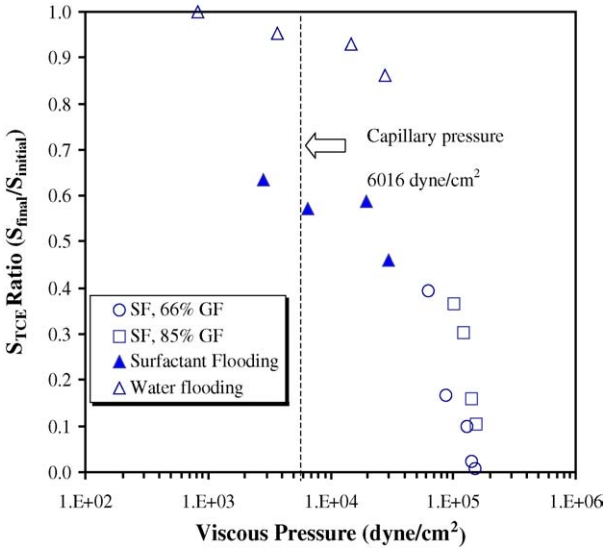

Fig. 5. Effect of the viscous pressure of the displacing fluid on TCE desaturation. The viscous pressure was calculated by Eq. (3) with the apparent viscosity.

SF flooding produced a higher viscous pressure than surfactant flooding as shown in Fig. 1. The increased viscous pressures displayed a trend in the displacement of a higher amount of TCE. As noted earlier, the applied conditions of SF flooding and surfactant flushing were similar, but the produced conditions of the two floods were different. SF presented an increased viscous pressure contributing to the enhanced displacement of residual TCE.

4. Summary and implications

SF produced the higher viscous pressures than the viscous pressures expected from the properties of the constituents. The increased viscous pressure resulted in a higher desaturation of TCE trapped in the pores. Displacement of the residual TCE began as the viscous pressure of flood was closed to the capillary pressure of the porous medium. In the region of viscous pressure that was closed to the capillary pressure, visualization of floods clearly showed that residual TCE was either retained or solubilized, not displaced, implying that TCE solubilization was the dominant TCE removal process.

In a remediation system using surfactant solution, three different removal processes can be applied to the system: (1) reducing IFT for TCE mobilization; (2) increasing viscous forces for TCE displacement and (3) solubilizing TCE without mobilization or displacement. The results of the study indicate that a surfactant flood would be used for TCE solubilization rather than TCE mobilization or TCE displacement. The result of the study, Fig. 5 showed that surfactant and

water floods needed so high flood velocity to obtain a high TCE removal.

SF floods produced so high viscous pressures at the similar conditions to surfactant floods and resulted in the high TCE desaturations. Therefore, physical forces analysis prior to application would give us exact information on the dominant removal process under given application conditions. This study used a glass porous model and did not consider interactions between surfactant solution and soil. Further investigation on physical force variations with real site conditions, such as surfactant partitioning, permeability reduction and soil heterogeneity are required for extension of the study results.

References

[1] National Research Council, Alternatives for Ground Water Cleanup, National Academy Press, Washington DC, 1994.
[2] J.L. Wilson, S.H. Conrad, W.R. Mason, W. Peplinski, E. Hagan, Laboratory Investigation of Residual Liquid Organics from Spills, Leaks, and the Disposal of Hazardous Waste in Groundwater, USEPA, Ada, OK, 1990, EPA/600/6-90/004.
[3] K.D. Pennell, M. Jin, L.M. Abriola, G.A. Pope, Surfactant enhanced remediation of soil columns contaminated by residual tetrachloroethylene, J. Contam. Hydrol. 16 (1994) 35–53.
[4] J.C. Fountain, C. Waddell-Sheets, A. Lagowski, C. Taylor, D. Frazier, M. Byrne, Enhanced removal of dense non-aqueous phase liquids using surfactants, in: D.A. Sabatini, R.C. Knox, J.H. Harwell (Eds.), Surfactant-Enhanced Subsurface Remediation, American Chemical Society, Washington, DC, 1995, pp. 177–190.
[5] C.T. Miller, E.I. Hill, M. Moutier, Remediation of DNAPL-contaminated subsurface systems using density-motivated mobilization, Environ. Sci. Technol. 34 (2000) 719–724.
[6] K.E. Martel, R. Martel, R. Lefebvre, P.J. Gelinas, Laboratory study of polymer solutions used for mobility control during in situ NAPL recovery, Ground Water Monit. Rem. 18 (1998) 103–113.
[7] B.I. Longino, B.H. Kueper, Effects of capillary pressure and use of polymer solutions on dense, non-aqueous-phase liquid retention and mobilization in a rough-walled fracture, Environ. Sci. Technol. 33 (1999) 2447–2455.
[8] S.-W. Jeong, M.Y. Corapcioglu, S.E. Roosevelt, Micromodel study of surfactant foam remediation for residual trichloroethylene, Environ. Sci. Technol. 34 (2000) 3456–3461.
[9] L.W. Holm, The mechanism of gas and liquid flow through porous media in the presence of foam, SPEJ 8 (1968) 359–369.
[10] G.G. Bernard, L.W. Holm, W.L. Jacob, Effect of foam on trapped gas saturation and on permeability of porous media to water, SPEJ 5 (1965) 295–300.
[11] L. Minssiex, Oil displacement by foams in relation to their physical properties in porous media, J. Pet. Technol. 26 (1974) 100–108.
[12] A.H. Falls, J.J. Musters, R. Ratulowski, The apparent viscosity of foams in homogeneous bead packs, SPE Res. Eng. 4 (1989) 155–164.
[13] H.O. Lee, J.P. Heller, M.W. Hoefer, Change in apparent viscosity of CO_2-foam with rock permeability, in: SPE/DOE Seventh Symposium on Enhanced Oil Recovery, Tulsa, OK, 1990, pp SPE/DOE 20194.
[14] J. Bear, Dynamics of Fluids in Porous Media, Dover Publications, Inc., New York, 1972.
[15] R.A. Ettinger, C.J. Radke, Influence of texture on steady foam flow in berea sandstone, SPE Res. Eng. 7 (1992) 83–90.
[16] P.C. Persoff, C.J. Radke, K. Pruess, S.M. Benson, P.A. Witherspoon, A laboratory investigation of foam flow in sandstone at elevated pressure, SPE Res. Eng. 6 (1991) 365–372.
[17] R. Lenormand, E. Touboul, C. Zarcone, Numerical models and experiments on immiscible displacements in porous media, J. Fluid Mech. 189 (1988) 165–187.
[18] G.J. Hirasaki, J.B. Lawson, Mechanism of foam flow in porous media: apparent viscosity in smooth capillaries, SPEJ 25 (1985) 176–190.
[19] D.J. Manlowe, C.J. Radke, A pore-level investigation of foam/oil interactions in porous media, SPE Res. Eng. 5 (1990) 405–502.